only 2.4 mm × 1.4 mm, which is small enough for use in the inner ear and for approaching the small space around the RWN. The small diameter of such devices, however, exposes them to four potential problems—(1) low-quality images, (2) increased chance of clogging the channel with drug solution, (3) increased effort required to clean the channel, and (4) increased fragility—all of which we took into account during the development of our improved otoendoscope.

The otoendoscope system for inner ear drug delivery has the following features:

1. A 30-gauge needle attached to a catheter to remove or perforate RWN mucosal adhesions and to inject drugs (Fig. 1).
2. A catheter threaded inside the channel to deliver drug solutions so liquids never directly contact the working channel, preventing channel clogging.
3. An elliptical shape that enables our otoendoscopy device to more effectively capture the field in the light-guided area than prototype otoendoscopes, resulting in brighter and higher-quality images.

This modified otoendoscope has a similar bore as previous ones, but it is less fragile and less troublesome to use. We tested a conventional otoendoscope, a prototype otoendoscope, and the newly developed otoendoscope on cadaver temporal bones. Prior to using the drug delivery device, under otoendoscopy conventional myringotomy was performed with a small blade (2 mm) at the junction between the posteroinferior quadrants, and then the otoendoscope combined with a catheter was inserted into the inner ear.

All research was conducted with the approval of the Keio University Hospital Institutional Review Board and in accordance with the Helsinki Declaration. The novel otoendoscope inner ear drug delivery device is currently being developed for clinical use.

3. Results

We observed complete obstruction of the RWN in 2 of 5 cadaver temporal bones (Table 1). We also compared our otoendoscope with prototype (Machida Corporation, Tokyo Japan) or conventional otoendoscopes (Olympus Corporation Tokyo, Japan). After performing myringotomy, we used the three different types of otoendoscopes to view the RWM and found that our novel otoendoscope produced good-quality images of the RWM (Fig. 2A). However, because the lens contained within our otoendoscope is only 0.6 mm in diameter, image resolution was not as high-quality as that of the conventional otoendoscope we tested. Thus, the lens requires additional refinement. Although 30°-angled otoendoscopy is typically used to view the RWN, straight (0°) otoendoscopy

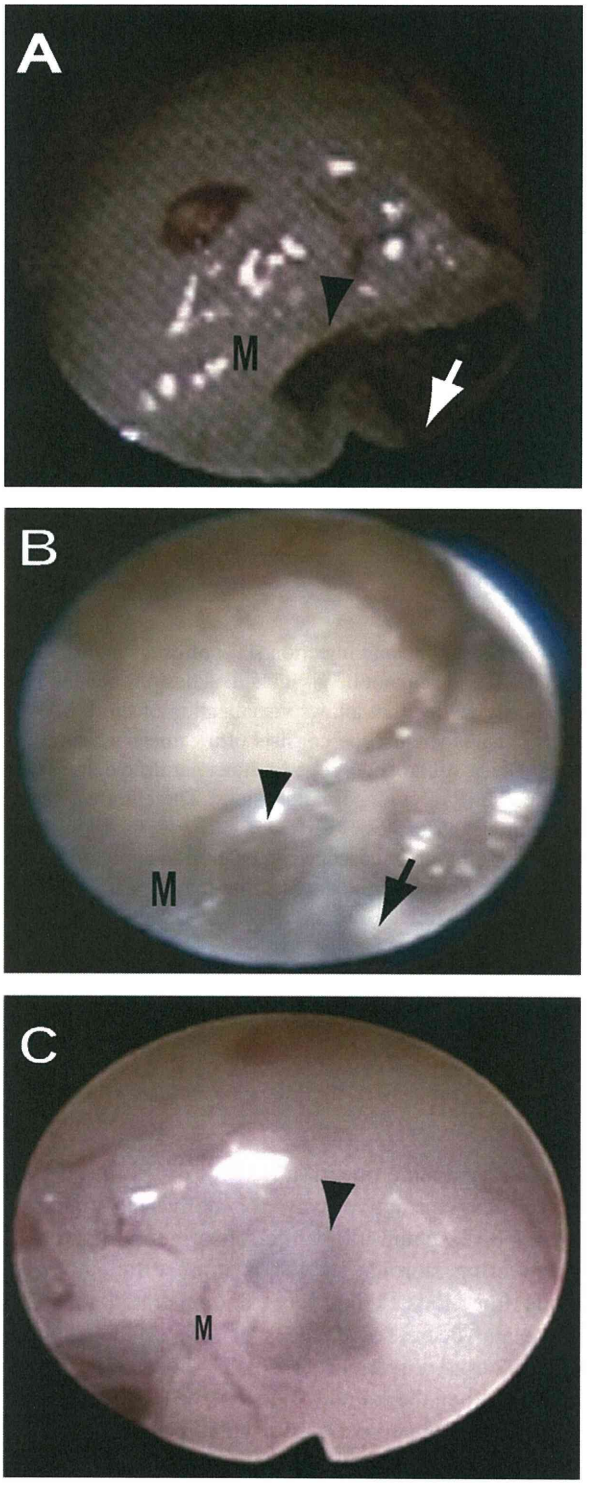

Fig. 1. Novel otoendoscope developed in our clinic. (A) Frontal view of the otoendoscope showing the lens (L) and two channels (W, working channel; *, suction channel). (B) Side view of the otoendoscope with catheter and needle. Scale bar: 5 cm. (C) High magnification view of the tip of the otoendoscope (E) showing the catheter (Ca) and needle (N). A catheter for angiography is also available for this scope. For inner ear procedures, a 30-gauge needle (*) is inserted into the tip of the catheter.

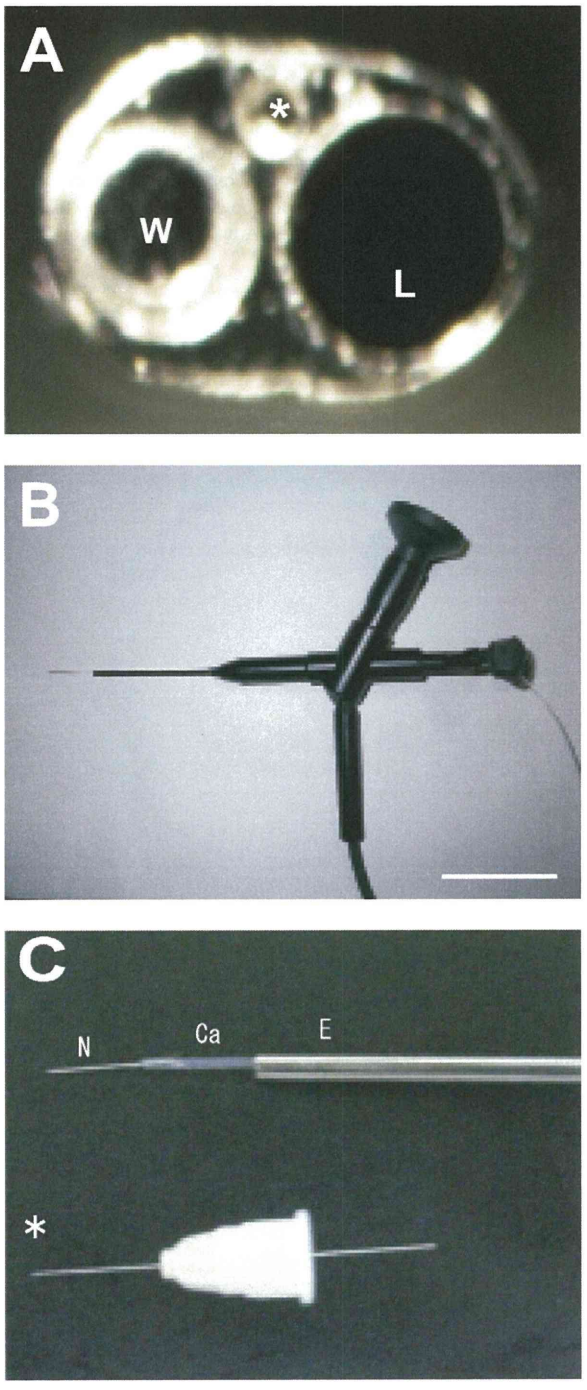

Fig. 2. Round window membrane (RWM indicated by "M" and arrowheads) images as visualized through different otoendoscopes. RWM images captured with the novel otoendoscope (A), a prototype otoendoscope (B), and a 30-angled (1.9 mm; Olympus) conventional otoendoscope (C). The image shown in panel C was especially of high quality. (A and B) Using a needle, we opened up the connective tissue overlying the RWN and injected a solution onto the RWM (M). The needles are indicated by arrows.

can also capture images of the RWM (Fig. 2). Because 0°-angled otoendoscopes are easier to handle, it may be easier to view RWM images through 0°-angled otoendoscopy than through 30°-angled otoendoscopy.

Table 1
RW obstruction of cadaver.

Case (age, sex)	Cadaver condition	RW obstruction
Unknown, F	Fixed	+
Unknown, F	Fixed	−
90 y/o, F	Unfixed	+
94 y/o, F	Unfixed	+/−
92 y/o, F	Unfixed	−

RWM obstruction +: present, +/−: partial present, −: not present.

Table 2
Comparison of different otoendoscopes.

	Results of comparison
Observation of RWM	C > N = P
Treatment of adhesions	N = C > P
Otoendoscope diameter (mm)	N(1.5) > C(1.9) > P(2.4)

C, conventional otoendoscope; N, novel otoendoscope with catheter; P, prototype otoendoscope with catheter.

4. Discussion

Our otoendoscope represents a new concept in treating and diagnosing inner ear-associated hearing loss. If ITI is unsuccessful, the RWM should be examined. This can be carried out conveniently with our otoendoscope. Additionally, our otoendoscope can be used also for diagnosing perilymphatic fistulas and for providing related therapy.

We compared the advantages and disadvantages of the novel otoendoscope, a prototype otoendoscope, and a conventional otoendoscope (Table 2). Although our otoendoscope is smaller than other types of otoendoscopes, it still captures an adequate image of the RWN. Moreover, our otoendoscope combined with a catheter can be used to evaluate the RWN before a local drug delivery system is put into place; to apply drugs directly onto the surface of the RWM; and to verify the correct placement of an inner ear drug delivery system, ensuring that it is safely in place.

Acknowledgements

We thank Mr. Ishikawa and his colleagues at Machida Corporation for helping develop the otoendoscope. This work was supported by grants from the Ministry of Health, Labor, and Welfare in Japan (H16-008 K.O. and S.K.), and Ministry of culture, sports, science and technology in Japan (20390444 K.O., R.T. and S.K.).

References

[1] Silverstein H, Choo D, Rosenberg SI, Kuhn J, Seidman M, Stein I, et al. Intratympanic steroid treatment of inner ear disease and tinnitus (preliminary report). Ear Nose Throat J 1996;75:468–71.

[2] Xenellis J, Papadimitriou N, Nikolopoulos T, Maragoudakis P, Segas J, Tzagaroulakis A, et al. Intratympanic steroid treatment in idiopathic sudden sensorineural hearing loss: a control study. Otolaryngol Head Neck Surg 2006;134:940–5.
[3] Sahni RS, Paparella MM, Schachern PA, Goycoolea MV, Le CT. Thickness of the human round window membrane in different forms of otitis media. Arch Otolaryngol Head Neck Surg 1987;113:630–4.
[4] Alzamil KS, Linthicum Jr FH. Extraneous round window membranes and plugs: possible effect on intratympanic therapy. Ann Otol Rhinol Laryngol 2000;109:30–2.
[5] Crane BT, Minor LB, Della Santina CC, Carey JP. Middle ear exploration in patients with Meniere's disease who have failed outpatient intratympanic gentamicin therapy. Otol Neurotol 2009;30:619–24.
[6] Plontke SK, Zimmermann R, Zenner HP, Lowenheim H. Technical note on microcatheter implantation for local inner ear drug delivery: surgical technique and safety aspects. Otol Neurotol 2006;27:912–7.
[7] Plontke SK, Plinkert PK, Plinkert B, Koitschev A, Zenner HP, Lowenheim H, et al. Transtympanic endoscopy for drug delivery to the inner ear using a new microendoscope. Adv Otorhinolaryngol 2002;59: 149–155.

Acta Oto-Laryngologica, 2011; 131: 628–632

informa
healthcare

ORIGINAL ARTICLE

Pure tone auditory thresholds can change according to duration of interrupted tones in patients with psychogenic hearing loss

NAOKI OISHI[1,2], YASUHIRO INOUE[1], AKEMI HORI[1], REIKO YAKUSHIMARU[1], NAOYUKI KOHNO[2] & KAORU OGAWA[1]

[1]*Department of Otolaryngology, Keio University School of Medicine, Tokyo and* [2]*Department of Otolaryngology, Head and Neck Surgery, Kyorin University School of Medicine, Tokyo, Japan*

Abstract

Conclusion: Pure tone auditory thresholds can change according to duration of interrupted tones in patients with mild to severe psychogenic hearing loss (PHL). *Objectives:* To examine how the duration of stimulus tones affects the hearing thresholds of patients with PHL. *Methods:* Twelve patients with PHL (21 ears) were enrolled in this study. We initially measured their hearing thresholds using interrupted tones with a duration of 2 s and equal length of on-time and off-time, 225 ± 35 ms, respectively. After a 10 min interval, we measured their hearing thresholds using the same interrupted tones conditions lasting 5 s. The average threshold gains (2 s thresholds minus 5 s thresholds) were compared to those of 15 control subjects with normal hearing (25 ears), 15 patients with cochlear hearing loss (23 ears), and 4 patients with retrocochlear lesions (4 ears). Patients with profound PHL (4 patients, 6 ears) were analyzed separately. *Results:* The average threshold gain of PHL patients (excluding profound PHL patients) at all frequencies was 18.3 dB, which was significantly larger than that of other groups: 0.3 dB (profound PHL patients), 3.8 dB (controls with normal hearing), 3.0 dB (patients with cochlear hearing loss), and 3.2 dB (patients with retrocochlear lesions).

Keywords: *Attention, loudness, short-term memory, audiogram*

Introduction

Psychogenic hearing loss (PHL) is defined as hearing loss that cannot be explained by anatomic or physiologic abnormalities and is differentiated from malingering and factitious disorder [1,2]. Many terms besides PHL have been used in the literature to describe the discrepancy between actual hearing thresholds and measured pure tone thresholds in the absence of organic disease: nonorganic hearing loss, pseudohypoacusis, conversion deafness, and functional hearing loss [3,4].

Many studies exist on the pure tone thresholds of PHL patients. The pure tone thresholds of PHL patients typically exhibit a 'saucer-shaped' audiometric configuration, which is considered to be a result of adherence to an equal-loudness standard [5]. The test–retest reliability of the pure tone audiometry is sometimes poor in PHL patients, and audiometric fluctuations often reveal to clinicians that the hearing loss is PHL [3]. It is also known that the duration of the stimulus tones may affect the audiogram results of patients with PHL. When patients with PHL listen to a sound lasting several seconds, some begin to respond gradually to the sound a few seconds after the sound starts, even though the loudness of the sound does not change. They typically express their feelings as follows: 'At first, the sound felt like it was coming from a far place. Then I started to notice the sound.'

Although this phenomenon is accepted as one of the characteristics in patients with PHL, to the best of our knowledge, no studies have determined how much the pure tone thresholds of audiograms may

Correspondence: Naoki Oishi MD, Department of Otolaryngology, Keio University School of Medicine, 35 Shinanomachi Shinjuku, Tokyo 160-8582, Japan. Tel: +81 3 5363 3827. Fax: +81 3 3353 1261. E-mail: o-ishi@mub.biglobe.ne.jp

(Received 19 September 2010; accepted 18 November 2010)

ISSN 0001-6489 print/ISSN 1651-2251 online
DOI: 10.3109/00016489.2010.543147

change according to the duration of tones. We hypothesize that pure tone auditory thresholds can change according to the duration of the stimulus tones in patients with PHL, irrespective of the severity of the PHL.

Material and methods

Twelve patients with PHL (21 ears exhibiting PHL) were enrolled in this study. These patients were evaluated and treated at the Hearing and Tinnitus Clinic of the Keio University Hospital. Of the 12 patients, 2 were men and 10 were women; age ranged from 15 to 71 years (median age 27 years). Of the 21 ears, 11 had left-sided PHL and 10 had right-sided PHL. The average auditory threshold at all frequencies tested (125, 250, 500, 1000, 2000, 4000, and 8000 Hz) of all the ears was 67.7 (SD 29.5) dBHL, which included six ears in the range of 21–40 dBHL (mild PHL), four ears in the range of 41–70 dBHL (moderate PHL), five ears in the range of 71–90 dBHL (severe PHL), and six ears in the range of 91–110 dBHL (profound PHL).

First, we measured the hearing thresholds using interrupted tones with a duration of 2 s and equal length of on-time and off-time, 225 ± 35 ms, respectively (2 s thresholds). These are standard parameters for pure tone audiometry in Japan [6]. After a 10 min interval, we obtained the other hearing thresholds using the same interrupted tones conditions lasting 5 s (5 s thresholds), which are 3 s longer than those used in the standard method. The average threshold gains (2 s thresholds minus 5 s thresholds) at all frequencies tested of the patients with PHL were compared to those of 15 controls with normal hearing (25 ears), 15 patients with cochlear sensorineural hearing loss (23 ears), and 4 patients with retrocochlear lesions (4 ears). Of the 15 controls, 7 were men and 8 were women; age ranged from 17 to 58 years (median age 32 years); average auditory threshold at all frequencies tested was 11.4 (SD 4.1) dBHL. Of the 15 patients with cochlear sensorineural hearing loss, 10 were men and 5 were women; age ranged from 34 to 79 years old (median age 67 years); average auditory threshold at all frequencies tested was 43.1 (SD 22.3) dBHL. Of the four patients with retrocochlear lesions, all were men; age ranged from 29 to 78 years (median age 54 years); average auditory threshold at all frequencies tested was 49.8 (SD 28.7) dBHL. The lesions of all four of these patients were vestibular schwannomas.

Patients with profound PHL (four patients, six ears) were analyzed separately from patients with mild to severe PHL, because the former barely responded to any sounds. Consequently, the remaining group of PHL patients comprised 8 patients (15 ears) with an average auditory threshold of 54.9 (SD 25.0) dBHL at all frequencies tested.

The diagnoses of PHL, cochlear hearing loss, or retrocochlear hearing loss depended on the following tests: pure tone audiometry, otoacoustic emissions (OAEs), auditory brain response (ABR), and magnetic resonance imaging (MRI) [7]. Normal hearing level in pure tone audiometry was defined as <30 dBHL at all frequencies measured. PHL patients frequently require a longer time to respond to the stimulus tones than subjects with normal hearing and patients with organic hearing loss, therefore it took a longer time to measure pure tone audiometry for PHL patients than for other subjects. All of the patients with PHL enrolled in this study had normal hearing function, indicated by OAE and ABR. Malingering and factitious disorder were carefully ruled out.

We obtained informed consent from all patients to have their hearing thresholds measured twice. However, considering possible increased attention to the stimuli that may be caused by explained instructions, especially in patients with PHL, the difference of the duration of interrupted tones between the two measurements was not referred to in the explanation of the test procedure.

The threshold gains between groups were statistically examined with analysis of variance (ANOVA) followed by the Bonferroni post hoc test. All significance tests were two-tailed and conducted at the 5% significance level. All statistics were calculated using JMP version 8.0.1 (SAS Institute Inc., Cary, NC, USA).

This study was approved by the Institutional Review Board at Keio University, School of Medicine.

Results

Representative case report

A 19-year-old woman came to our clinic because of bilateral hearing loss. Pure tone audiometry revealed bilateral sensorineural hearing loss (Figure 1); however, there was a discrepancy between the patient's ability to converse and her measured hearing level. We performed distortion-product and transient-evoked OAEs (DPOAEs and TEOAEs, respectively) and ABR tests on the patient, which revealed normal hearing function for both her ears (Figures 2 and 3). We noted that she experienced much daily stress from family problems. Her symptoms and test results led us to diagnose PHL. Next, we performed pure tone audiometry using different tone durations, as described above. The tests showed significant hearing

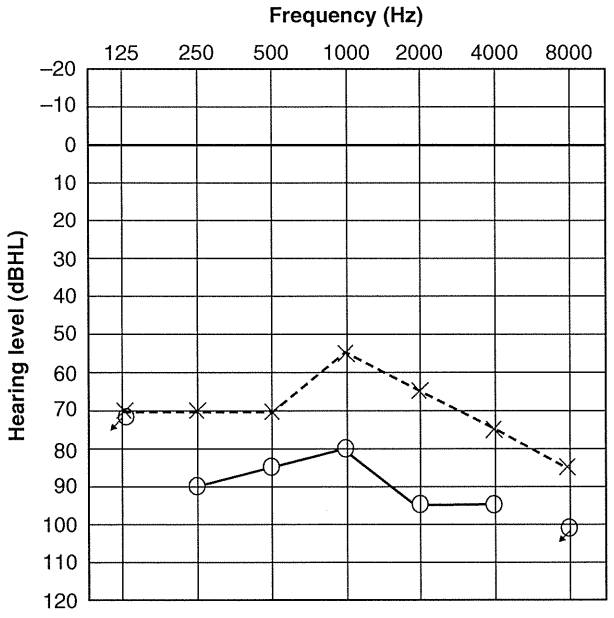

Figure 1. Pure tone audiometry results for a 19-year-old patient with psychogenic hearing loss. Hearing thresholds were measured by using the interrupted tones with a duration of 2 s and the equal length of on-time and off-time, 225 ± 35 ms, respectively.

gains for both of her ears when the tests were performed with interrupted tones lasting for 5 s versus those lasting for 2 s (Figure 4).

Results for all the cases

The average threshold gain of 8 patients with PHL (15 ears), excluding those with profound PHL, at all frequencies tested was 18.3 (SD 13.7) dB, which was significantly larger than that of other groups ($p < 0.01$, ANOVA): 0.7 (SD 1.2) dB in patients with profound PHL; 4.6 (SD 2.4) dB in controls with normal hearing; 3.1 (SD 3.1) dB in patients with cochlear hearing loss; and 3.2 (SD 2.2) dB in patients with retrocochlear lesions (Figure 5). The average threshold gain of patients with PHL did not differ according to the measured frequencies. Patients with PHL presenting with profound hearing loss barely responded to any tone, regardless of the duration of interrupted tones. There were no differences between normal controls, patients with cochlear lesions, and patients with retrocochlear lesions.

Discussion

The results of this study indicate that pure tone auditory thresholds can change according to the duration of interrupted tones in patients with mild to severe PHL. Our study also suggests that patients presenting with profound PHL barely responded to any tone, regardless of the duration of interrupted tones.

The absolute thresholds of sounds depend on durations of the sounds [8]. For durations less than ~200 ms, the sound intensity necessary for detection increases as duration of the sound decreases; on the other hand, for durations exceeding ~500 ms, the sound intensity necessary for detection is independent of duration of the sound. This mechanism for sound detection cannot explain the hearing improvement observed in the patients with PHL in the present study. We consistently used the interrupted tones of which on-time was 225 ± 35 ms, and varied only the total length of the interrupted tones from 2 to 5 s, which resulted in improved response to tones in

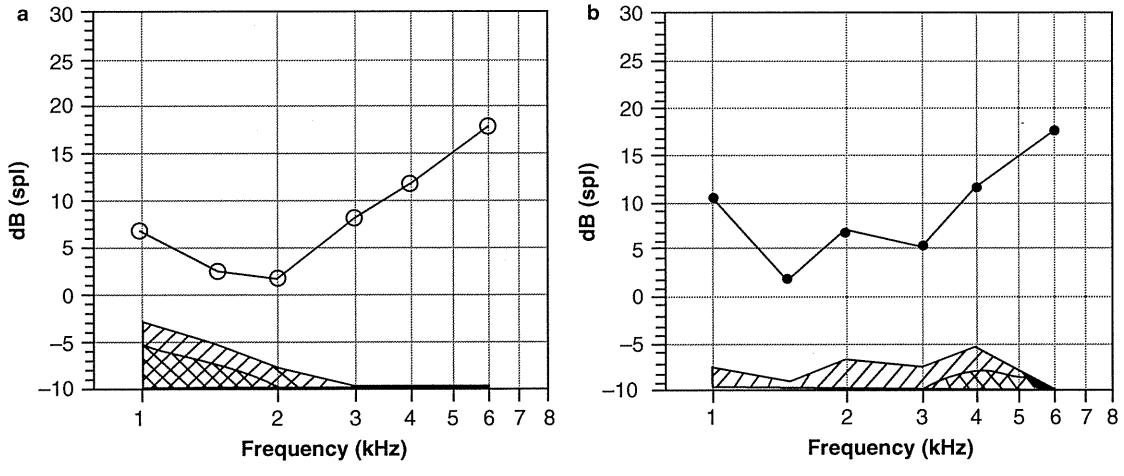

Figure 2. Distortion-product otoacoustic emission (DPOAE) results for a 19-year-old patient with psychogenic hearing loss. (a) Right ear, (b) left ear. Function of outer hair cells in both ears was normal.

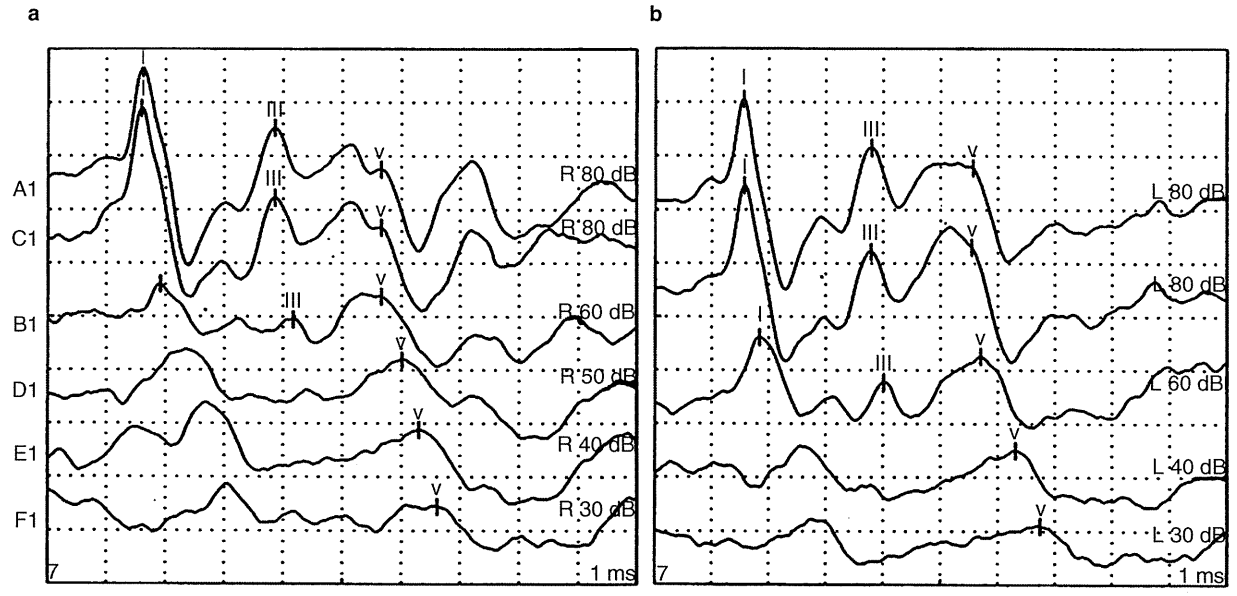

Figure 3. Auditory-brain response results for a 19-year-old patient with psychogenic hearing loss. (a) Right ear, (b) left ear. V waves were observed in both ears following 30 dB stimulation. This was not consistent with the patient's pure tone audiometry results (see Figure 1).

patients with PHL. Thus, we need to consider other mechanisms that may underlie the sound duration-related hearing improvement in patients with PHL.

In patients with PHL, hearing thresholds typically show a saucer-shaped audiometric configuration [5], and Bekesy audiograms are typically type V [9,10].

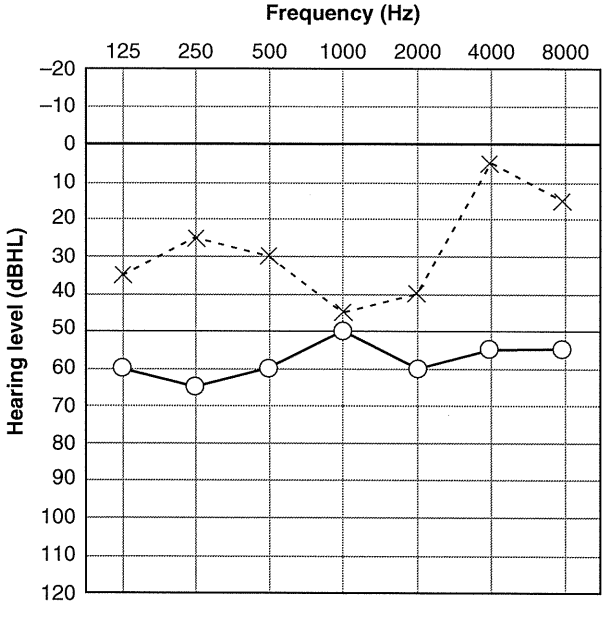

Figure 4. Pure tone audiometry results for a 19-year-old patient with psychogenic hearing loss. Hearing thresholds were measured by using interrupted tones with a duration of 5 s and equal length of on-time and off-time, 225 ± 35 ms, respectively. In comparison with the thresholds evoked by relatively shorter 2 s tones (see Figure 1), the thresholds evoked by longer 5 s tones showed significant improvement. These tests were performed at an interval of 10 min.

Both patterns are considered to be a result of adherence to an equal-loudness standard in the patients' memory [5,11]. Although it is not known why patients with PHL judge the loudness of sounds by tracing their memory, memory seems to play an important role in determining auditory thresholds in these patients.

Another characteristic audiometric phenomenon in patients with PHL is observed during 'suggestion audiometry,' a test procedure used to detect nonorganic hearing loss and to determine the actual healing levels of a patient [12]. In this test, a tester 'suggests' to a patient that wearing a hearing aid would improve his/her hearing. However, unbeknownst to the patient, the hearing aid is switched off during the pure tone audiometry. In children with PHL, this type of 'suggestion' protocol improved the auditory thresholds of the children [12]. These authors provided an explanation for this phenomenon, proposing that the 'suggestion' improves attention in children with attention deficits, which in turn improves the children's ability to detect sounds. Findings by Hosoi et al. [12] complement those of another study, which reported that attention deficit may affect the N100 m findings of auditory-evoked fields in patients with PHL [13]. They observed attenuation of the N100 m amplitude in 5 PHL patients but not in 10 control patients. Together, these findings indicate that attention may also play an important role in determining auditory thresholds in patients with PHL.

Models exist that describe the relationship between attention and awareness [14]. One model posits that

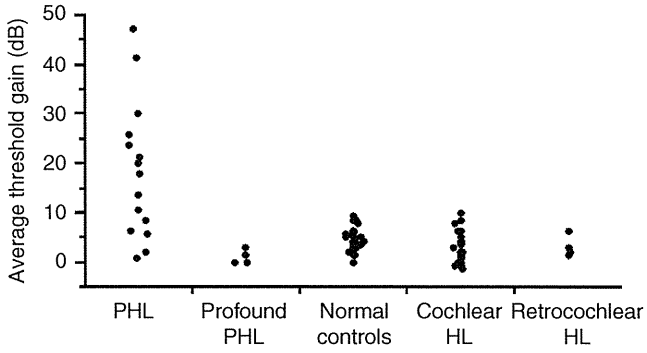

Figure 5. Distribution of average threshold gains at all frequencies tested of all the subjects. Threshold gains were calculated by subtracting 5 s threshold values from 2 s threshold values. The subjects were classified into 5 groups: PHL, PHL patients excluding profound PHL patients (8 cases, 15 ears); profound PHL (4 cases, 6 ears); normal control, controls with normal hearing (15 cases, 25 ears); cochlear HL, patients with cochlear sensorineural hearing loss (15 cases, 23 ears); and retrocochlear HL, patients with retrocochlear lesions (4 cases, 4 ears). The average threshold gain of the PHL group was significantly larger than that of other groups ($p < 0.01$, ANOVA). PHL, psychogenic hearing loss; HL, hearing loss.

sensory inputs are analyzed and gated by attention into awareness, which can prompt the subject to react to the sensory information. This model can be applied to our present results. The 5 s tones may attract more attention than the 2 s tones, which makes the patients more aware of the tones and thus improves the patients' reaction to the tones. Another model considers sensory input and memory [14], such that information about sensory inputs is moved into short-term memory via the attention process. Short-term memory is one of the key steps in the neural mechanisms underlying auditory discrimination of long-duration tones [15]. This concept can also be applied to our results. The increased attention caused by the 5 s tones causes the 'sound' information to move into the patients' short-term memory; and when the loudness of the sound matches the loudness in the patients' long-term memory, the PHL patients can react to the sound.

In this study, we analyzed patients with mild to severe PHL separately from patients with profound PHL, because the latter patients barely responded to any sound, regardless of the duration of the interrupted tones. Although it is unclear whether a different mechanism underlies the hearing loss in patients with profound PHL, our results indicated that enhancing attention in patients with profound PHL does not improve their auditory thresholds. Considering the rare incidence of profound PHL [16], it may be necessary to consider that profound PHL may have a different etiology than mild to severe PHL.

Declaration of interest: The authors report no conflicts of interest. The authors alone are responsible for the content and writing of the paper.

References

[1] Austen S, Lynch C. Non-organic hearing loss redefined: understanding, categorizing and managing non-organic behaviour. Int J Audiol 2004;43:449–57.
[2] Lin J, Staecker H. Nonorganic hearing loss. Semin Neurol 2006;26:321–30.
[3] Rintelmann WF, Schwan SA, Blakley BW. Pseudohypacusis. Otolaryngol Clin North Am 1991;24:381–90.
[4] Wolf M, Birger M, Ben Shoshan J, Kronenberg J. Conversion deafness. Ann Otol Rhinol Laryngol 1993;102:349–52.
[5] Doerfler LG. Psychogenic deafness and its detection. Ann Otol Rhinol Laryngol 1951;60:1045–8; discussion 60–71.
[6] Tsuiki T, Ota F. Auditory function tests [chokakukensahou]. Audiology Japan 1990;33:793–806 (in Japanese).
[7] Oishi N, Kanzaki S, Kataoka C, Tazoe M, Takei Y, Nagai K, et al. Acute-onset unilateral psychogenic hearing loss in adults: report of six cases and diagnostic pitfalls. ORL J Otorhinolaryngol Relat Spec 2009;71:279–83.
[8] Moore BCJ. 2003. An introduction to the psychology of hearing. 5th edition. London: Academic Press.
[9] Jerger J, Herer G. Unexpected dividend in Bekesy audiometry. J Speech Hear Disord 1961;26:390–1.
[10] Stein L. Some observations on type V Bekesy tracings. J Speech Hear Res 1963;13:339–48.
[11] Hattler KW. The type V bekesy pattern: the effects of loudness memory. J Speech Hear Res 1968;11:567–76.
[12] Hosoi H, Tsuta Y, Murata K, Levitt H. Suggestion audiometry for non-organic hearing loss (pseudohypoacusis) in children. Int J Pediatr Otorhinolaryngol 1999;47:11–21.
[13] Sakamoto M, Itasaka Y, Ishikawa K. [N100 m findings of auditory-evoked fields in patients with psychogenic hearing impairment.] Nippon Jibiinkoka Gakkai Kaiho 2007;110: 672–9 (in Japanese).
[14] Gazzaniga MS, Davies G, Ivry RB, Mangun GR. 2008. Cognitive neuroscience: the biology of the mind. 3rd International student edition. New York: WW Norton & Co.
[15] Ulloa A, Husain FT, Kemeny S, Xu J, Braun AR, Horwitz B. Neural mechanisms of auditory discrimination of long-duration tonal patterns: a neural modeling and fMRI study. J Integr Neurosci 2008;7:501–27.
[16] Tsuiki T. [Hearing test for psychogenic hearing loss.] Audiology Japan 2008;51:253–62 (in Japanese).

THYROID RESEARCH

RESEARCH Open Access

Influence of dietary iodine deficiency on the thyroid gland in *Slc26a4*-null mutant mice

Tomoyuki Iwata[1,2], Tadao Yoshida[1], Masaaki Teranishi[1], Yoshiharu Murata[3], Yoshitaka Hayashi[3], Yasuhiko Kanou[3], Andrew J Griffith[4] and Tsutomu Nakashima[1*]

Abstract

Background: Pendred syndrome (PDS) is an autosomal recessive disorder characterized by sensorineural hearing impairment and variable degree of goitrous enlargement of the thyroid gland with a partial defect in iodine organification. The thyroid function phenotype can range from normal function to overt hypothyroidism. It is caused by loss-of-function mutations in the *SLC26A4* (*PDS*) gene. The severity of the goiter has been postulated to depend on the amount of dietary iodine intake. However, direct evidence has not been shown to support this hypothesis. Because *Slc26a4*-null mice have deafness but do not develop goiter, we fed the mutant mice a control diet or an iodine-deficient diet to evaluate whether iodine deficiency is a causative environmental factor for goiter development in PDS.

Methods: We evaluated the thyroid volume in histological sections with the use of three-dimensional reconstitution software, we measured serum levels of total tri-iodothyronine (TT3) and total thyroxine (TT4) levels, and we studied the thyroid gland morphology by transmission electron microscopy.

Results: TT4 levels became low but TT3 levels did not change significantly after eight weeks of an iodine-deficient diet compared to levels in the control diet animals. Even in *Slc26a4*-null mice fed an iodine-deficient diet, the volume of the thyroid gland did not increase although the size of each epithelial cell increased with a concomitant decrease of thyroid colloidal area.

Conclusions: An iodine-deficient diet did not induce goiter in *Slc26a4*-null mice, suggesting that other environmental, epigenetic or genetic factors are involved in goiter development in PDS.

Background

Pendred syndrome (PDS) is an autosomal recessive disorder characterized by sensorineural hearing impairment, presence of goiter, and a partial defect in iodine organification [1]. The goiter in PDS is variable in its presentation; it can develop at any age (although generally after puberty), but may be totally absent in some affected individuals [2]. Also, there is substantial intrafamilial and regional variation, and nutritional iodine intake may be a significant modifier of the thyroid phenotype [1]. Kopp *et al.* suggested that under conditions of sufficient iodine intake, thyroid enlargement may be very mild or absent, and hence these patients are often simply categorized as having enlarged vestibular aqueduct [1]. Sato *et al.* also suggested that even in patients with impaired iodide transport, high iodine intake may prevent the development of goiter [3].

Slc26a4-null (*Slc26a4*$^{-/-}$) mutant mice were generated by Everett *et al.* [2]. *Slc26a4*$^{-/-}$ mice are profoundly deaf with vestibular dysfunction, but they lack goiter and thyroid histological abnormalities. We hypothesized that the absence of goiter and hypothyroidism in *Slc26a4*$^{-/-}$ mice was due to a sufficient iodine intake, and that goiter and hypothyroidism might be induced by iodine deficiency. We, therefore, performed this study to investigate the influence of iodine intake on serum thyroid hormone levels and the histology and volume of the thyroid gland in *Slc26a4*$^{-/-}$ mice.

Materials and methods

Slc26a4-null mice

An *Slc26a4*-null (*Slc26a4*$^{-/-}$) mouse colony was established and bred with homozygotes and heterozygotes imported from the National Institutes of Health

* Correspondence: tsutomun@med.nagoya-u.ac.jp
[1]Department of Otorhinolaryngology Nagoya University Graduate School of Medicine, 65 Tsurumai-cho, Showa-ku, Nagoya, Aichi 466-8550, Japan
Full list of author information is available at the end of the article

(Rockville, Maryland) [2]. The line was maintained on a 129/SvEv background.

Breeding and Diet

Matings were performed between *Slc26a4*$^{-/-}$ and *Slc26a4*$^{-/-}$, and between *Slc26a4*$^{+/-}$ and *Slc26a4*$^{+/-}$ mice. These mice were fed a control diet (CLEA Japan Inc.). F1 offspring at two months of age were paired for mating. The mice were fed iodine-deficient chow (CLEA Japan Inc. T-08514) or control chow (CLEA Japan Inc. T-08513) from the beginning of the mating. Each chow was comprised solely of artificial materials. According to an analysis by the Laboratories for Food & Environmental Science, Tokyo, Japan, the iodine level was less than the sensing threshold (< 0.02 mg%) in iodine-deficient chow (ICD) whereas it was 0.51 mg% in control chow (CCD). F2 offspring were fed with the same diet as their parents for 12 to 16 weeks after weaning. *Slc26a4* genotyping was performed on DNA prepared from tail specimens obtained at the time of sacrifice of the mice. There were six groups comprising one of three different genotypes (*Slc26a4*$^{-/-}$, *Slc26a4*$^{+/-}$, and *Slc26a4*$^{+/}$) and either of ICD or CCD. Thirty-one 12 to 16 week-old males were used for this study (Table 1). Females were not analyzed in order to avoid the effect of menstrual cycles on hormone levels. The experimental protocol was approved by the Experimental Animal Management Committee, Nagoya University, Graduate School of Medicine.

Serum thyroid hormones

After deep anesthesia by intraperitoneal injection of pentobarbital sodium, blood was collected from the inferior vena cava. Serum total tri-iodothyronine (TT3) and total thyroxine (TT4) levels were measured by an electrochemiluminescence immunoassay (TT3: DRG® T-3 ELISA, TT4: DRG® T-4 ELISA, DRG International, East Mountainside, New Jersey USA).

Thyroid histology and volume

After intracardiac infusion of 4% paraformaldehyde, thyroid glands were excised together with adjacent tracheae and immersed in the same fixative for 24 hours at 4°C. The specimens were placed in 10% EDTA for seven days, washed with phosphate buffered saline (PBS), embedded in paraffin, and sectioned at 4-μm thickness for collection of every fifth section. The sections were stained with hematoxylin-eosin. The serial sections were observed with a light microscope system (BZ-8000, Keyence, Tokyo, Japan) and saved as digital images. A digital image of the whole thyroid was reconstructed and the volume was measured using three-dimensional reconstruction software, ZedView (LEXI, Tokyo, Japan).

Ultrastructural evaluation

One mouse was selected randomly for electron microscopic observation of the thyroid gland from each group of *Slc26a4*$^{-/-}$ CCD, *Slc26a4*$^{-/-}$ ICD, *Slc26a4*$^{+/-}$CCD and *Slc26a4*$^{+/-}$ ICD. The electron microscopic observation was done according to the method described previously [4]. Two-mm^3 thyroid specimens were excised, fixed in 2.5% glutaraldehyde for 24 hours at 4°C, washed in 0.1M phosphate buffer (pH = 7.0), and fixed again in 1% osmium tetroxide for 3 hours at 4°C. The samples were dehydrated in a graded series of ethanol and embedded in epoxy resin. Ultrathin sections were cut, double stained with uranyl acetate and lead citrate, and examined using a JEOL JEM100S electron microscope (JEOL, Tokyo, Japan).

Statistics

Statistical analysis was performed using SPSS Statistics ver.19.0 (SPSS Inc., Chicago, IL). One-way ANOVA and Mann-Whitney U-testing were used for statistical analysis. A *P* value less than 0.05 defined a significant difference.

Results

Volume of thyroid gland

The thyroid volume in each animal is shown in Table 1. Mean thyroid volumes of *Slc26a4*$^{-/-}$, *Slc26a4*$^{+/-}$ and *Slc26a4*$^{+/+}$ mice fed with CCD were 1.8 ± 1.0 mm^3, 1.9 ± 0.9 mm^3, 1.4 ± 0.2 mm^3 respectively. The mean thyroid volumes of *Slc26a4*$^{-/-}$, *Slc26a4*$^{+/-}$ and *Slc26a4*$^{+/+}$ mice fed with ICD were 1.0 ± 0.3 mm^3, 1.5 ± 0.6 mm^3, 1.1 mm^3 respectively. There were no significant differences in mean thyroid volumes between ICD and CCD groups for any genotype. The thyroid images reconstructed by three-dimensional reconstruction software are shown in Figure 1.

Histological findings

Figure 2 demonstrates light microscopic observation of the thyroid gland of ICD and CCD groups for the three different *Slc26a4* genotypes. The size and height of epithelial cells increased with a concomitant decrease of colloidal area in ICD thyroid glands as compared to those of CCD animals among all genotypes. Electron microscopic observations in *Slc26a4*$^{-/-}$ and *Slc26a4*$^{+/-}$ thyroid glands were consistent with these findings (Figure 3).

Serum thyroid hormone levels

Serum concentrations of TT3 and TT4 in each animal are shown in Table 1. In the CCD group, the average TT3 levels were 1.26 μg/dl, 1.39 μg/dl and 1.53 μg/dl in *Slc26a4*$^{-/-}$, *Slc26a4*$^{+/-}$ and *Slc26a4*$^{+/+}$ mice, respectively. In the ICD group, the average TT3 levels were 0.92 μg/dl, 0.93 μg/dl and 1.07 μg/dl in *Slc26a4*$^{-/-}$, *Slc26a4*$^{+/-}$ and

Table 1 Total tri-iodothyronine (TT3) and total thyroxine (TT4) levels and thyroid volumes in *Slc26a4*-null mice eating control chow (CCD) or iodine-deficient chow (ICD)

Genotype	Diet	Body weight (g)	TT3 (ng/ml)	TT4 (μg/dl)	Volume (mm^3)
Slc26a4$^{-/-}$	CCD	25.6	2.80	8.70	0.95
		22.5	1.24	5.10	1.03
		19.8	0.74	4.68	EM
		28.9	0.76	3.99	2.27
		29.7	0.78	3.78	2.93
	ICD	25.4	0.87	3.60	0.67
		22.5	0.79	3.58	1.28
		21.3	0.99	2.77	0.88
		23.0	1.01	3.52	1.28
		20.9	0.86	3.42	0.75
		25.7	1.04	3.12	1.07
		24.6	0.88	1.79	EM
Slc26a4$^{+/-}$	CCD	25.6	1.30	6.30	1.48
		23.8	1.35	5.90	1.47
		23.5	1.45	4.03	1.28
		27.4	2.40	8.10	1.03
		28.2	1.60	5.05	2.82
		25.1	0.82	3.83	EM
		38.0	0.81	4.13	3.22
	ICD	24.8	1.02	4.29	1.31
		23.4	0.84	3.11	0.66
		29.2	0.87	2.64	EM
		33.3	0.82	2.41	2.04
		31.7	1.12	2.92	1.92
Slc26a4$^{+/+}$	CCD	26.8	1.55	3.97	1.63
		24.5	1.60	3.88	1.44
		23.7	2.10	8.40	1.38
		25.0	1.60	5.95	1.31
		26.7	0.79	3.45	1.24
	ICD	23.4	0.93	4.26	1.11
		23.8	1.20	4.35	UM

EM, examined with electron microscopy.

UM, unmeasurable due to failure to prepare adequate thin sections.

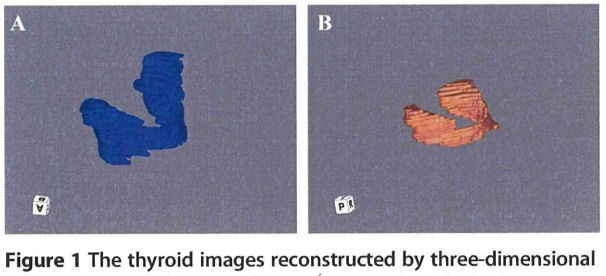

Figure 1 The thyroid images reconstructed by three-dimensional reconstruction software. A, *Slc26a4*$^{-/-}$ mouse thyroid with iodine-deficient chow (ICD) (reconstructed with three-dimensional software, Zed View). B, *Slc26a4*$^{-/-}$ mouse thyroid with control chow (CCD) (reconstructed with three-dimensional software, Zed View).

Slc26a4$^{+/+}$ mice, respectively. The average TT4 levels in the CCD group were 5.25 μg/dl, 5.33 μg/dl and 5.13 μg/dl in *Slc26a4*$^{-/-}$, *Slc26a4*$^{+/-}$ and *Slc26a4*$^{+/+}$ mice, respectively. The average TT4 levels in the ICD group were 3.11 μg/dl, 3.07 μg/dl and 4.31 μg/dl in *Slc26a4*$^{-/-}$, *Slc26a4*$^{+/-}$ and *Slc26a4*$^{+/+}$ mice, respectively. One-way ANOVA did not reveal a significant difference in TT3 and TT4 levels among the three genotypes.

As shown in Figure 4, Mann-Whitney U-testing revealed that serum TT4 level was lower in the ICD group than in the CCD group both in *Slc26a4*$^{-/-}$ and *Slc26a4*$^{+/-}$ mice (p = 0.004 and p = 0.019, respectively). In *Slc26a4*$^{+/+}$ mice, Mann-Whitney U-testing was not

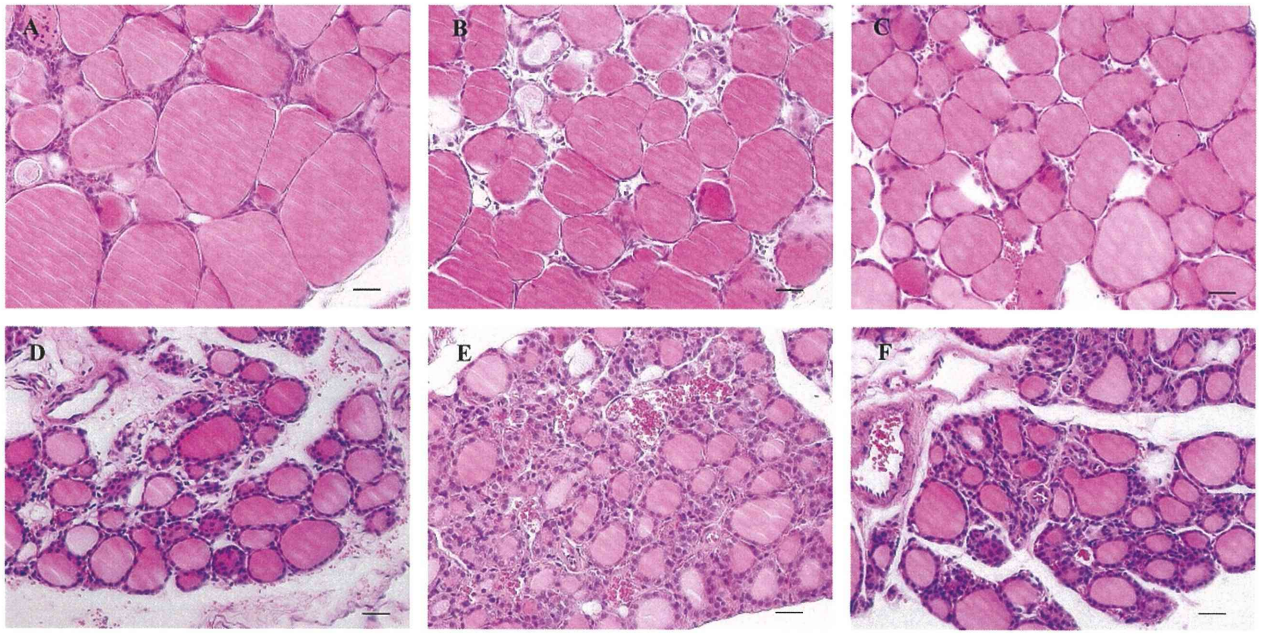

Figure 2 Light microscopic findings of the thyroid gland. A, *Slc26a4*$^{-/-}$ control chow (CCD); B, *Slc26a4*$^{+/-}$ CCD; C, *Slc26a4*$^{+/+}$ CCD; D, *Slc26a4*$^{-/-}$ iodine-deficient chow (ICD); E, *Slc26a4*$^{+/-}$ ICD; F, *Slc26a4*$^{+/+}$ ICD. Scale bars: 30 μm.

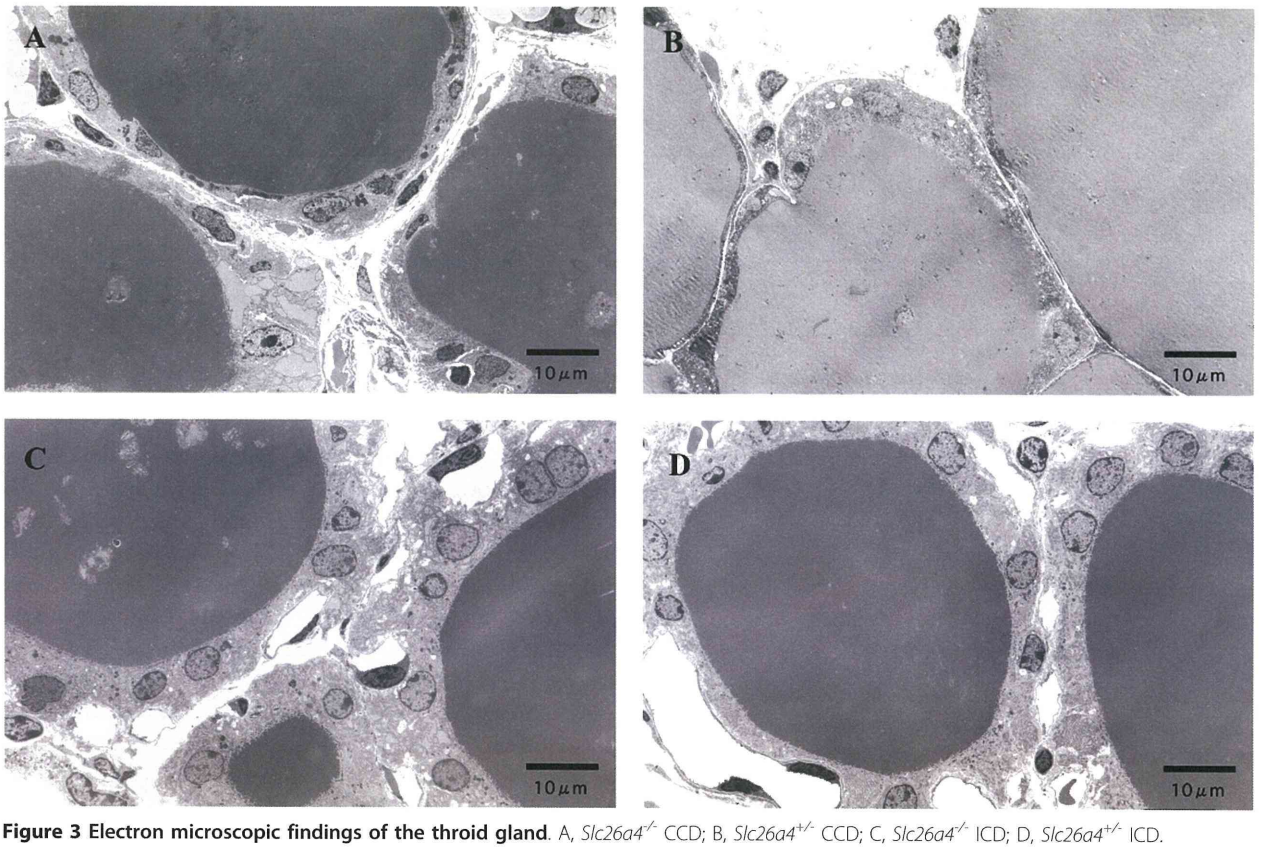

Figure 3 Electron microscopic findings of the throid gland. A, *Slc26a4*$^{-/-}$ CCD; B, *Slc26a4*$^{+/-}$ CCD; C, *Slc26a4*$^{-/-}$ ICD; D, *Slc26a4*$^{+/-}$ ICD.

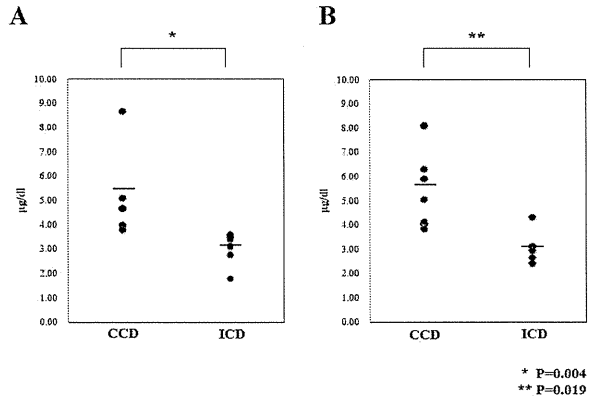

Figure 4 Effect of iodine deficiency on serum total thyroxine (TT4) levels in Slc26a4$^{-/-}$ and Slc26a4$^{+/-}$ mice. A, TT4 levels of Slc26a4$^{-/-}$ mice among control chow (CCD) and iodine-deficient chow (ICD) groups. B, TT4 levels of Slc26a4$^{+/-}$ mice among CCD and ICD groups. Mann-Whitney U-testing indicated significant differences for both comparisons.

adequate to compare between ICD group and CCD group because the number of ICD animals was two. On the other hand, the TT3 level was not different significantly between the ICD and CCD groups.

Discussion

Mutations of the *SLC26A4* (*PDS*) gene can cause sensorineural hearing loss with goiter (PDS) or non-syndromic recessive deafness with enlarged vestibular aqueduct [5,6]. To date, more than 150 mutations in the *SLC26A4* gene have been reported in patients with PDS or nonsyndromic deafness with enlarged vestibular aqueducts (http://www.healthcare.uiowa.edu/labs/pendredandbor/slcMutations.htm). According to previous reports, the H723R missense substitution accounts for up to 75% of *SLC26A4* mutations in Japanese families with EVA [6,7]. There are many cases without goiter associated with the H723R mutation [3]. Madeo *et al.* found that thyroid gland volume is primarily *SLC26A4* genotype-dependent in children but is age-dependent in adults [8]. These reports suggest that the variable degree of thyroid dysfunction and goiter associated with *SLC26A4* mutations may be caused by factors unrelated to *SLC26A4* genotype. It is noteworthy that reported homozygotes for the H723R mutation were mainly from Japan and Korea where daily iodine intake should be comparatively high [3,7,9]. We therefore hypothesized that the amount of iodine intake influences the thyroid phenotype associated with PDS, leading us to study the effect of dietary iodine deficiency on thyroid gland structure and function in *Slc26a4*-null mutant mice.

TT4 levels were lower in the ICD group than in the CCD group. This difference was observed regardless of genotype, and these results suggest the thyroid function of *Slc26a4*$^{-/-}$ mice is approximately the same as of *Slc26a4*$^{+/-}$ and *Slc26a4*$^{+/+}$ mice. While we were preparing the manuscript, we found a similar report by Calebiro *et al* [10]. In their report they also confirmed that dietary iodine restriction did not induce goiter in *Slc26a4*$^{-/-}$ mice. However, Calebiro *et al.* reported that total TT4 levels did not differ significantly between mice fed a low-iodine diet in comparison to those fed a standard diet [10].

The reason why TT3 levels did not decrease might be because incompletely iodinated thyroglobulin (Tg) in the thyroid colloid is accompanied by an increase in monoiodotyrosine (MIT) on Tg molecules, resulting in preferential T3 synthesis [11]. Therefore, TT3 levels may have been maintained despite the decline in TT4 levels in iodine-deficient mice. Another explanation why TT3 was unchanged in mice fed an iodine-deficient diet is an increase of type 1 iodothyronine 5'-deiodinase (D1) activity in the thyroid gland. Pedraza *et al.* reported that thyroidal D1 activity was increased with an iodine-deficient diet [12].

Other factors may compensate for defective iodine transport in both patients with PDS and *Slc26a4*$^{-/-}$ mice. Van den Hove *et al.* have reported that the ClCn5 (chloride channel 5) protein localizes at the apical membrane of thyrocytes. The thyroidal phenotype in ClCn5-deficient mice is similar to that in Pendred syndrome, suggesting that ClCn5 could participate in mediating apical iodine efflux or iodine/chloride exchange [13,14]. Suzuki *et al.* reported that thyroglobulin, by mediating differential expression of several thyroid-specific genes including *TSHR*, *NIS*, and *TPO*, *TG*, *PAX8*, *TTF1*, and *TTF2* regulates the rate of iodide efflux into the follicular lumen and may thus play an important role in regulating thyroid function under constant levels of TSH [13,15].

In conclusion, the ICD did not induce goiter in *Slc26a4*-null mice whereas, in humans, *SLC26A4* mutations sometimes lead to goiter and even hypothyroidism. Mice may be different from humans in their ability to transport iodide into the follicular lumen or mice may respond differently to altered iodine availability. It is also possible that our results result from the use of male experimental animals since goiter and hypothyroidism are more prevalent among human females than males. The genetic strain background may also influence the penetrance and expressivity of the thyroid phenotype associated with *Slc26a4* mutations. These may be some of the factors involved in the development of goiter in PDS.

Acknowledgements

This study was supported by research grants from the Ministry of Health, Labor, and Welfare and from the Ministry of Education, Culture, Sports, Science, and Technology of Japan. *Slc26a4*-null mice were kindly provided by NIH. Andrew Griffith was supported by NIH intramural research fund Z01-DC-000060.

Author details
[1]Department of Otorhinolaryngology Nagoya University Graduate School of Medicine, 65 Tsurumai-cho, Showa-ku, Nagoya, Aichi 466-8550, Japan. [2]Inazawa City Hospital, 1-1 Gokusho-cho, Inazawa, Aichi 492-8510, Japan. [3]Department of genetics, Research Institute of Environmental Medicine, Nagoya University, Furo-cho, Chikusa-ku, Nagoya, Aichi 464-8601, Japan. [4]National Institute on Deafness and Other Communications Disorders, National Institutes of Health, 5 Research Court, Rockville, MD 20850 USA.

Authors' contributions
TI designed and coordinated the study, performed the experiments and drafted the manuscript; TY and MT supervised all experimental procedures, participated in performing experiments, and helped to draft the manuscript; YM participated in coordination of the study and helped to draft the manuscript; YH participated in performing experiments. YK participated in coordination of the study. TN and AJG, the senior author, drafted the manuscript. All authors have read and approved the final manuscript.

Competing interests
The authors declare that they have no competing interests.

Received: 24 February 2011 Accepted: 20 June 2011
Published: 20 June 2011

References

1. Kopp P, Pesce L, Solis-S J: **Pendred syndrome and iodide transport in the thyroid.** *Trends Endocrinol Metab* 2008, **19**:260-268.
2. Everett L, Belyantseva I, Noben-Trauth K, Cantos R, Chen A, Thakkar S, Hoogstraten-Miller S, Kachar B, Wu D, Green E: **Targeted disruption of mouse Pds provides insight about the inner-ear defects encountered in Pendred syndrome.** *Hum Mol Genet* 2001, **10**:153-161.
3. Sato E, Nakashima T, Miura Y, Furuhashi A, Nakayama A, Mori N, Murakami H, Naganawa S, Tadokoro M: **Phenotypes associated with replacement of His by Arg in the Pendred syndrome gene.** *Eur J Endocrinol* 2001, **145**:697-703.
4. Kanou Y, Hishinuma A, Tsunekawa K, Seki K, Mizuno Y, Fujisawa H, Imai T, Miura Y, Nagasaka T, Yamada C, Ieiri T, Murakami M, Murata Y: **Thyroglobulin gene mutations producing defective intracellular transport of thyroglobulin are associated with increased thyroidal type 2 iodothyronine deiodinase activity.** *J Clin Endocrinol Metab* 2007, **92**:1451-1457.
5. Everett LA, Glaser B, Beck JC, Idol JR, Buchs A, Heyman M, Adawi F, Hazani E, Nassir E, Baxevanis AD, Sheffield VC, Green ED: **Pendred syndrome is caused by mutations in a putative sulphate transporter gene (PDS).** *Nat Genet* 1997, **17**:411-422.
6. Usami S, Abe S, Weston M, Shinkawa H, Van Camp G, Kimberling W: **Non-syndromic hearing loss associated with enlarged vestibular aqueduct is caused by PDS mutations.** *Hum Genet* 1999, **104**:188-192.
7. Kitamura K, Takahashi K, Noguchi Y, Kuroishikawa Y, Tamagawa Y, Ishikawa K, Ichimura K, Hagiwara H: **Mutations of the Pendred syndrome gene (PDS) in patients with large vestibular aqueduct.** *Acta Otolaryngol* 2000, **120**:137-141.
8. Manichaikul A, Reynolds J, Sarlis NJ, Pryor SP, Shawker T, Griffith AJ: **Evaluation of the thyroid in patients with hearing loss and enlarged vestibular aqueducts.** *Arch Otolaryngol Head Neck Surg* 2009, **135**:670-676.
9. Park H-J, Shaukat S, Liu X-Z, Hahn SH, Naz S, Ghosh M, Kim H-N, Moon S-K, Abe S, Tukamoto K, Riazuddin S, Kabra M, Erdenetungalag R, Radnaabazar J, Khan S, Pandya A, Usami S-I, Nance WE, Wilcox ER, Riazuddin S, Griffith AJ: **Origins and frequencies of SLC26A4 (PDS) mutations in east and south Asians: global implications for the epidemiology of deafness.** *J Med Genet* 2003, **40**:242-248.
10. Calebiro D, Porazzi P, Bonomi M, Lisi S, Grindati A, De Nittis D, Fugazzola L, Marinò M, Bottà G, Persani L: **Absence of primary hypothyroidism and goiter in Slc26a4 (-/-) Mice Fed on a Low Iodine Diet.** *J Endocrinol Invest* 2010.
11. Delange F: **The disorders induced by iodine deficiency.** *Thyroid* 1994, **4**:107-128.
12. Pedraza PE, Obregon MJ, Escobar-Morreale HF, del Rey FE, de Escobar GM: **Mechanisms of adaptation to iodine deficiency in rats: thyroid status is tissue specific. Its relevance for man.** *Endocrinology* 2006, **147**:2098-2108.
13. Bizhanova A, Kopp P: **Genetics and phenomics of Pendred syndrome.** *Mol Cell Endocrinol* 2010, **322**:83-90.
14. van den Hove M, Croizet-Berger K, Jouret F, Guggino S, Guggino W, Devuyst O, Courtoy P: **The loss of the chloride channel, ClC-5, delays apical iodide efflux and induces a euthyroid goiter in the mouse thyroid gland.** *Endocrinology* 2006, **147**:1287-1296.
15. Suzuki K, Kohn LD: **Differential regulation of apical and basal iodide transporters in the thyroid by thyroglobulin.** *J Endocrinol* 2006, **189**:247-255.

doi:10.1186/1756-6614-4-10
Cite this article as: Iwata *et al.*: Influence of dietary iodine deficiency on the thyroid gland in *Slc26a4*-null mutant mice. *Thyroid Research* 2011 4:10.

Acta Oto-Laryngologica, 2011; 131: 474–479

informa
healthcare

ORIGINAL ARTICLE

Endolymphatic hydrops and blood–labyrinth barrier in Ménière's disease

MITSUHIKO TAGAYA[1,3], MASAHIRO YAMAZAKI[2], MASAAKI TERANISHI[1], SHINJI NAGANAWA[2], TADAO YOSHIDA[1], HIRONAO OTAKE[1], SEIICHI NAKATA[1,4], MICHIHIKO SONE[1] & TSUTOMU NAKASHIMA[1]

[1]*Department of Otorhinolaryngology, Graduate School of Medicine, Nagoya University, Nagoya, Aichi,* [2]*Department of Radiology, Graduate School of Medicine, Nagoya University, Nagoya, Aichi,* [3]*Department of Otorhinolaryngology, Tosei General Hospital, Seto, Aichi and* [4]*Department of Otorhinolaryngology, Second Hospital, Fujita Health University School of Medicine, Nagoya, Aichi, Japan*

Abstract

Conclusions: The blood–labyrinth barrier is impaired in association with the hydrops grade in Ménière's disease. *Objectives:* To investigate the relationship between endolymphatic hydrops and the clinical characteristics of patients with Ménière's disease revealed by 3 T magnetic resonance imaging (MRI). *Methods:* A double dose of gadoteridol (Gd; 0.2 mmol/kg) was injected intravenously in 12 patients with Ménière's disease. We performed three-dimensional fluid attenuated inversion recovery MRI and three-dimensional real inversion recovery MRI 4 h later using a 3 T MRI unit. Ten patients had unilateral and two had bilateral Ménière's disease. *Results:* Fourteen ears with Ménière's disease showed intense Gd contrast on MRI compared with that in the 10 asymptomatic contralateral ears of patients with unilateral Ménière's disease (1.12 ± 0.36 vs 0.82 ± 0.15). The hydrops grade was correlated significantly with the contrast effect. The 14 ears with Ménière's disease had endolymphatic hydrops. Of the 10 contralateral ears of patients with unilateral Ménière's disease, 2 had endolymphatic hydrops in the cochlea and 6 had endolymphatic hydrops in the vestibule.

Keywords: *3 T magnetic resonance imaging, three-dimensional fluid attenuated inversion recovery, 3D FLAIR, contrast effect, signal intensity ratio, contralateral ear*

Introduction

Ménière's disease is an inner ear disorder with various recurrent symptoms, such as fluctuating hearing loss, tinnitus, and vertigo. It has been reported that Ménière's disease is related to pathological endolymphatic hydrops of the inner ear, but endolymphatic hydrops is also occasionally observed in the asymptomatic contralateral ear [1,2].

Because an ordinary amount of gadoteridol (Gd) intravenous injection is often insufficient to acquire enough contrast enhancement of inner ear, we injected a double dose of Gd to obtain clear inner ear magnetic resonance imaging (MRI) [3,4]. The advantage of intravenous Gd injection is very useful for the evaluation of bilateral Ménière's disease. In this study, we investigated the relationship between endolymphatic hydrops revealed with 3 T MRI and the clinical characteristics of Ménière's disease. We also evaluated the blood–labyrinth barrier in ears with and without Ménière's disease.

Material and methods

Patients

Twelve patients with Ménière's disease were enrolled in this study (Table I), including three previously reported patients [3]. Patient no. 10 had undergone surgery for acoustic neurinoma of her right ear when aged 58 years and had lost the hearing in her right ear completely. Our group previously reported that

Correspondence: Mitsuhiko Tagaya MD, Department of Otorhinolaryngology, Graduate School of Medicine, Nagoya University, 65 Tsurumai, Showa, Nagoya, Aichi 466–8550, Japan. Fax: +81 52 744 2325. E-mail: mi-man@ra2.so-net.ne.jp

(Received 7 September 2010; accepted 18 October 2010)

ISSN 0001-6489 print/ISSN 1651-2251 online
DOI: 10.3109/00016489.2010.534114

Table I. Patients' clinical characteristics.

Case no.	Gender	Age (years)	Side	Hearing fluctuation	Vertigo attacks	Low frequency hearing level at worse and better (dB)	Hearing level at 1000 Hz at worse and better (dB)	High frequency hearing level at worse and better (dB)	Time from onset of symptoms (months)	AAO–HNSclassification
1	M	41	Right	Yes	Rotatory	45, 25	15, 15	27, 17	61	Definite
			Left	No		15, 10	5, 5	10, 10		
2	F	67	Right	Yes	Rotatory	75, 68	60, 60	70, 60	6	Definite
			Left	No		22, 25	10, 10	10, 10		
3	M	68	Right	Yes	Rotatory	50, 25	25, 15	70, 57	2	Definite
			Left	No		27, 23	10, 10	43, 30		
4	M	36	Right	No	Rotatory	20, 17	10, 10	23, 17	28	Definite
			Left	Yes		67, 38	60, 30	45, 33		
5	F	42	Right	No	Rotatory	15, 15	10, 5	12, 5	78	Definite
			Left	Yes		20, 15	10, 10	12, 12		
6	F	46	Right	Yes	Rotatory	57, 42	85, 75	90, 90	48	Definite
			Left	Yes		33, 35	55, 50	82, 80		
7	M	62	Right	Yes	Rotatory	60, 50	45, 50	58, 57	1	Probable
			Left	No		27, 25	15, 20	55, 65		
8	M	38	Right	Yes	Rotatory	32, 20	10, 20	5, 8	1	Probable
			Left	Yes		25, 25	25, 25	7, 7		
9	F	74	Right	No	Rotatory	40, 47	55, 50	80, 78	20	Probable
			Left	Yes		50, 45	60, 50	72, 68		
10	F	60	Right	No	Nonrotatory	90, 90	110, 110	107, 107	8	Possible
			Left	Yes		87, 77	85, 60	90, 80		
11	F	36	Right	Yes	Nonrotatory	28, 22	30, 10	45, 17	1	Possible
			Left	No		15, 20	10, 10	5, 7		
12	M	55	Right	Yes	Nonrotatory	25, 20	20, 20	57, 50	30	Possible
			Left	No		23, 22	15, 15	43, 40		

Low frequency hearing level: average at 125, 250, and 500 Hz. High frequency hearing level: average at 2000, 4000, and 8000 Hz. Patient no. 10 had had an acoustic neurinoma of her right ear and the hearing data were excluded from the analysis. F, female; M, male.

increased permeability of the blood–labyrinth barrier in acoustic neurinoma [5]. Therefore, we excluded the hearing data and signal intensity ratio (SIR) for her right ear from our analysis in this study. Ménière's disease was diagnosed according to the criteria of the 1995 American Academy of Otolaryngology–Head and Neck Surgery (AAO–HNS) [6].

MRI

A double dose (0.4 ml/kg, 0.2 mmol/kg) of gadoteridol (ProHance®; Eisai, Tokyo, Japan) was injected intravenously. Four hours later, an MRI was performed using a 3 T MRI unit with a 32-channel array coil to obtain a high signal-to-noise ratio [4,7]. Heavily T2-weighted three-dimensional (3D) constructive interference in steady-state imaging was obtained for anatomical reference and 3D fluid attenuated inversion recovery (3D FLAIR) MRI was then performed to detect perilymph enhancement while suppressing the signal from the endolymph. Finally, we carried out 3D real inversion recovery MRI to visualize the endolymph, perilymph, and bone separately on a single image. The details of the MRI protocol have been described previously [3,4,8].

Image evaluation of the endolymphatic space

Gd administered intravenously enters the perilymph but does not enter the endolymph. The difference makes it possible to visualize the endolymphatic space. The degrees of endolymphatic hydrops in the vestibule and cochlea were classified into three groups: none, mild, and significant, according to the criteria described previously [9]. A radiologist who

was blinded to the patients' clinical data evaluated the hydrops grade. Example images are shown in Figure 1.

Evaluation of Gd contrast effects

The contrast effects on the cochlear fluid were evaluated semiquantitatively. This method has been reported previously in patients with sudden deafness [4]. The SIR was measured three times and the average SIR value was calculated for each ear. The results of simple SIR measurements have been reported to correlate well with those based on a quantitative method [10].

Ethics review

The protocol for the study was approved by the Ethics Review Committee of the Nagoya University School of Medicine (approval nos 369, 369–2, 369–3, and 369–4). All patients gave their informed consent to their participation in this study. Their written informed consent was attached to their electronic medical records after permission was obtained from the patients.

Statistical analysis

The data were analyzed with SPSS 17.0 for Windows (SPSS Inc., Chicago, IL, USA). Differences in SIR were assessed with the Mann–Whitney U test and those in categorical variables were assessed with the χ^2 test. Spearman's correlation coefficient was used to investigate the relationship between hearing level or SIR and hydrops grade (none 0, mild 1, significant 2). A p value of < 0.05 was considered statistically significant.

Results

The clinical characteristics of the 12 patients are shown in Table I. Ten patients had unilateral Ménière's disease and two had bilateral disease. All patients had hearing fluctuations in at least one ear. The worst mean low frequency hearing levels in the diseased ears and contralateral ears were 46.7 ± 20.7 dB and 22.7 ± 8.1 dB, respectively. The mean worst hearing levels at 1000 Hz in the diseased ears and contralateral ears were 41.8 ± 26.1 dB and 15.6 ± 15.1 dB, respectively. The mean worst high frequency hearing levels in the diseased ears and contralateral ears were 52.1 ± 29.7 dB and 31.2 ± 25.6 dB, respectively. The differences in the hearing levels of the diseased and contralateral ears at low frequencies and 1000 Hz were significant but these differences were not significant at high frequencies. According to the AAO–HNS classification, six patients were diagnosed with definite Ménière's disease. Three patients had fluctuating hearing loss with rotatory vertigo, but without definitive episodes of vertigo (probable Ménière's disease). Three patients had fluctuating hearing loss with nonrotatory vertigo (possible

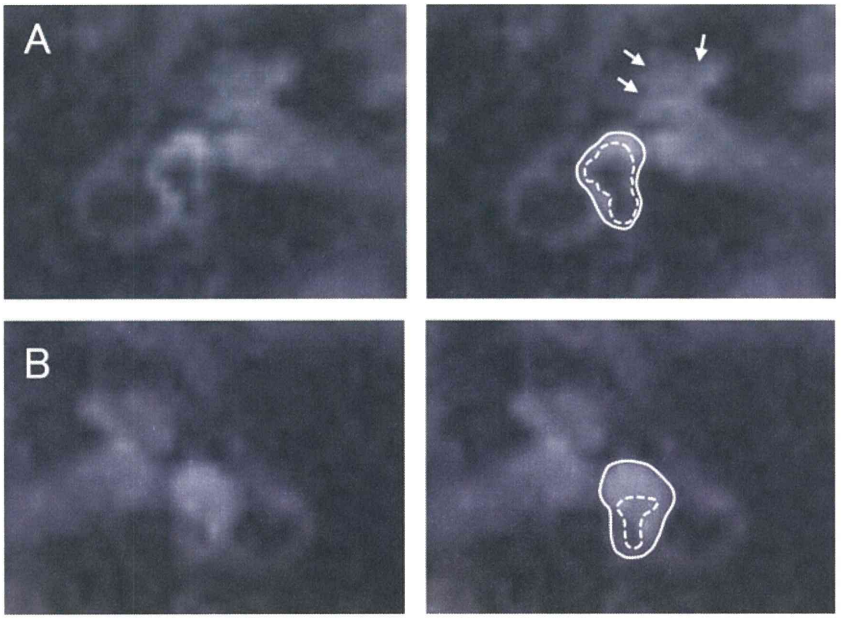

Figure 1. 3D FLAIR MRI of patient no. 3. Significant hydrops was observed in the cochlea (arrows) and vestibule of the diseased ear (A). The dotted line indicates the endolymphatic space and the solid line indicates the total fluid space in the vestibule. No hydrops was visible in the cochlea or vestibule of the contralateral ear (B).

Table II. Imaging data for each patient.

Case no.	Side	Diseased ear	Cochlear hydrops	Vestibular hydrops	SIR
1	Right	○	Significant	Significant	2.18
	Left		None	None	0.55
2	Right	○	Significant	Significant	1.33
	Left		None	Mild	1.04
3	Right	○	Significant	Significant	1.00
	Left		None	None	0.88
4	Right		None	Mild	0.65
	Left	○	Significant	Significant	0.71
5	Right		Mild	Mild	0.83
	Left	○	Significant	Significant	1.00
6	Right	○	None	Significant	0.99
	Left	○	None	Significant	0.93
7	Right	○	None	Significant	1.05
	Left		None	Mild	0.74
8	Right	○	None	Significant	0.94
	Left	○	Mild	Mild	0.81
9	Right		Mild	Mild	0.97
	Left	○	Significant	Significant	1.27
10	Right		None	None	2.79*
	Left	○	Significant	Significant	1.09
11	Right	○	Significant	Significant	1.44
	Left		None	None	0.88
12	Right	○	None	Mild	0.93
	Left		None	Significant	0.84

SIR, signal intensity ratio between the basal turn and cerebellar hemisphere.
*Patient no. 10 had had an acoustic neurinoma of her right ear and the SIR data were excluded from the analysis.

Ménière's disease). Table II shows the imaging data for each patient.

Of the 14 diseased ears, 8 showed significant hydrops (57%) and 1 mild hydrops (7%) in the cochlea, and 12 showed significant hydrops (86%) and 2 mild hydrops (14%) in the vestibule (Table III). Thus, the diseased ears showed hydrops in either the cochlea or vestibule. In the 10 contralateral ears, 2 showed mild hydrops (20%) in the cochlea and 1 showed significant hydrops (10%) and 5 mild hydrops (50%) in the vestibule. The diseased ears had more significant hydrops than the contralateral ears, in both the cochlea and vestibule.

The 14 ears with Ménière's disease had intense Gd contrast on MRI compared with that in the 10 contralateral ears in the patients with unilateral Ménière's disease (Figure 2; 1.12 ± 0.36 vs 0.82 ± 0.15).

The low frequency hearing level correlated significantly with the hydrops grade in the cochlea ($r = 0.448$) and vestibule ($r = 0.682$; Figure 3). The hearing level at 1000 Hz also correlated significantly with the hydrops grade in the cochlea ($r = 0.434$) and vestibule ($r = 0.605$). The high frequency hearing level was not related to the hydrops grade in the cochlea, but it was related to the hydrops grade in the vestibule ($r = 0.470$). SIR correlated with the hydrops grade in

Table III. Grading of hydrops in diseased ear and contralateral ear.

Parameter	Diseased ear	Contralateral ear	*p* value*
Number	14	10	
Cochlear hydrops			
Significant	8 (57%)	0 (0%)	0.019
Mild	1 (7%)	2 (20%)	
None	5 (36%)	8 (80%)	
Vestibular hydrops			
Significant	12 (86%)	1 (10%)	0.001
Mild	2 (14%)	5 (50%)	
None	0 (0%)	4 (40%)	

*χ^2 test.

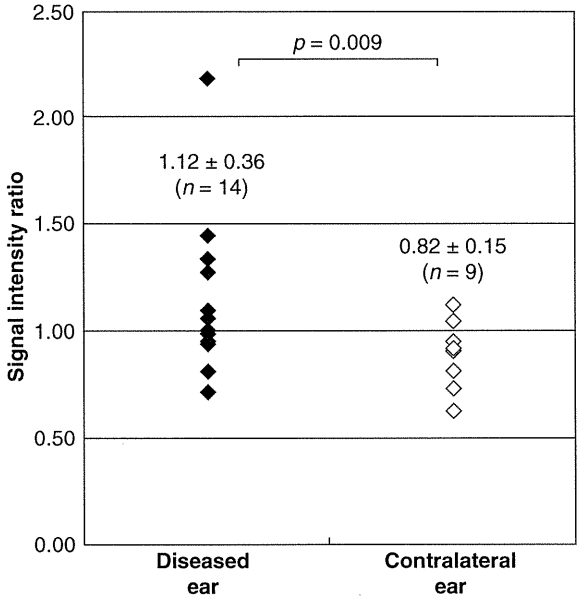

Figure 2. ◆ indicates the signal intensity ratio (SIR) of the diseased ear and ◇ indicates the SIR of the contralateral ear. The differences are statistically significant.

both the cochlea (r = 0.514) and the vestibule (r = 0.595; Figure 3). The hydrops grade in the diseased ears did not differ between the 11 ears with rotatory vertigo and the 3 ears with nonrotatory vertigo in the cochlea or vestibule.

Discussion

This is the first report to demonstrate the clinical characteristics of patients with Ménière's disease and endolymphatic hydrops visualized with MRI. The diseased ears had significant hydrops, in either the cochlea or vestibule, with an intense contrast effect. The hydrops grade correlated with the hearing level at low frequencies and 1000 kHz, but was not associated with the rotatory or nonrotatory type of vertigo. The contralateral ear often had hydrops but without symptoms. The hydrops grade and the contrast effect were also correlated significantly.

Ménière's disease is characterized by endolymphatic hydrops, which has been conventionally confirmed with temporal bone pathology. However, in

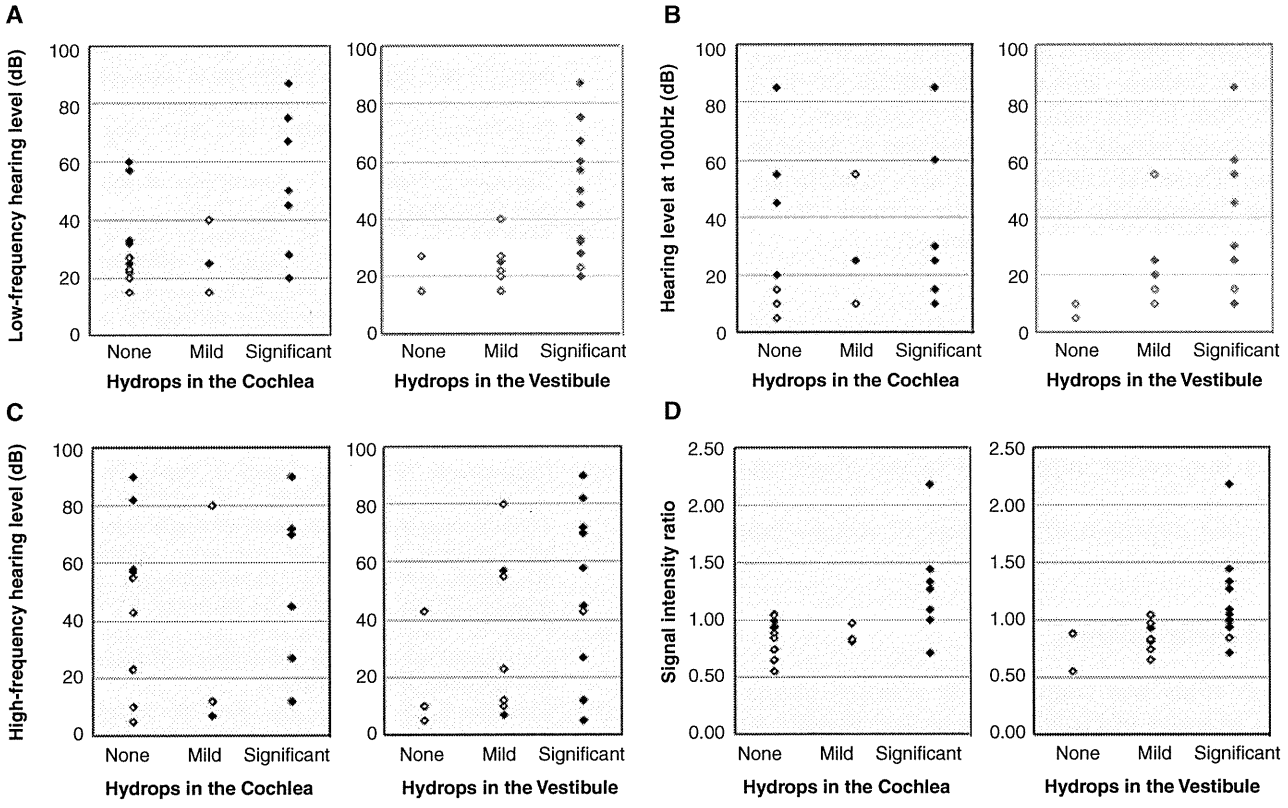

Figure 3. The scatter graph shows the relationship between the hearing level or signal intensity ratio (SIR) and the hydrops grade. ◆ indicates the diseased ear and ◇ the contralateral ear. (A) The low frequency hearing level was correlated significantly with hydrops in the cochlea and vestibule. (B) The hearing level at 1000 Hz was also correlated significantly with hydrops in the cochlea and vestibule. (C) The high frequency hearing level was not correlated with the hydrops in the cochlea, but it was correlated with the hydrops in the vestibule. (D) SIR was correlated significantly with the hydrops grade in both the cochlea and the vestibule.

the clinical setting, a practical diagnosis and treatment are required, based on a few clinical examinations. MRI is a useful tool for the correct diagnosis and choice of treatment in living human beings.

Histopathological examinations of the temporal bone revealed that the contralateral ears of patients with unilateral Ménière's disease had asymptomatic saccular hydrops in 35% [1] and 37.5% of patients [2]. Our results show that hydrops was present in 2 of 10 cochleas and in 6 of 10 vestibules in the asymptomatic ears of patients with Ménière's disease. Because by our definitional criterion, the hydrops grade was evaluated from the area ratio, hydrops may have been overdiagnosed in the vestibule [9]. In future, the evaluation of endolymphatic hydrops by volume may be necessary when advanced MRI techniques are used.

Individuals with disabling longstanding unilateral disease are not likely to develop bilateral disease [11]. Moreover, Reissner's membrane from the temporal bone shows similar cellular densities in patients with endolymphatic hydrops with or without Ménière's disease [12]. Therefore these studies suggest that pathophysiological mechanisms other than hydrops may be responsible for the symptoms of Ménière's disease. The intense contrast effect seen in our study indicates that the blood–labyrinth barrier is impaired in ears with Ménière's disease. The correlation between endolymphatic hydrops and the permeability of the blood–labyrinth barrier indicated increasing permeability of the blood vessels in the progression to Ménière's disease. These MRI findings indicate a relationship enamong dolymphatic hydrops, the clinical symptoms of Meniere's disease and its etiology.

Conclusion

Our study revealed that the blood–labyrinth barrier is impaired in association with hydrops grade in Ménière's disease. Because the intravenous Gd injection may reveal impairment of the blood–labyrinth barriers, the intravenous Gd injection has potential for the fine detection of pathology of various inner ear diseases.

Acknowledgments

This study was supported by research grants from the Ministry of Health, Labour and Welfare and the Ministry of Education, Culture, Sports, Science and Technology in Japan.

Declaration of interest: The authors report no conflicts of interest. The authors alone are responsible for the content and writing of the paper.

References

[1] Lin MY, Timmer FC, Oriel BS, Zhou G, Guinan JJ, Kujawa SG, et al. Vestibular evoked myogenic potentials (VEMP) can detect asymptomatic saccular hydrops. Laryngoscope 2006;116:987–92.

[2] Morita N, Kariya S, Farajzadeh Deroee A, Cureoglu S, Nomiya S, Nomiya R, et al. Membranous labyrinth volumes in normal ears and Ménière disease: a three-dimensional reconstruction study. Laryngoscope 2009;119: 2216–20.

[3] Nakashima T, Naganawa S, Teranishi M, Tagaya M, Nakata S, Sone M, et al. Endolymphatic hydrops revealed by intravenous gadolinium injection in patients with Meniere's disease. Acta Otolaryngol 2010;130: 338–43.

[4] Tagaya M, Teranishi M, Naganawa S, Iwata T, Yoshida T, Otake H, et al. 3 Tesla magnetic resonance imaging obtained 4 hours after intravenous gadolinium injection in patients with sudden deafness. Acta Otolaryngol 2010;130: 665–9.

[5] Yamazaki M, Naganawa S, Kawai H, Nihashi T, Fukatsu H, Nakashima T. Increased signal intensity of the cochlea on pre- and post- contrast enhanced 3D-FLAIR in patients with vestibular schwannoma. Neuroradiology 2009;51: 855–63.

[6] Committee on Hearing and Equilibrium guidelines for the diagnosis and evaluation of therapy in Meniere's disease. American Academy of Otolaryngology–Head and Neck Foundation, Inc. Otolaryngol Head Neck Surg 1995;113: 181–5.

[7] Naganawa S, Nakashima T. Cutting edge of inner ear MRI. Acta Otolaryngol Suppl 2009;560:15–21.

[8] Naganawa S, Sugiura M, Kawamura M, Fukatsu H, Sone M, Nakashima T. Imaging of endolymphatic and perilymphatic fluid at 3T after intratympanic administration of gadolinium-diethylene-triamine pentaacetic acid. AJNR Am J Neuroradiol 2008;29:724–6.

[9] Nakashima T, Naganawa S, Pyykko I, Gibson WP, Sone M, Nakata S, et al. Grading of endolymphatic hydrops using magnetic resonance imaging. Acta Otolaryngol Suppl 2009; 560:5–8.

[10] Naganawa S, Ishihara S, Iwano S, Kawai H, Sone M, Nakashima T. Estimation of gadolinium-induced T1-shortening with measurement of simple signal intensity ratio between the cochlea and brain parenchyma on 3D-FLAIR: correlation with T1 measurement by TI scout sequence. Magn Reson Med Sci 2010;9:17–22.

[11] Perez R, Chen JM, Nedzelski JM. The status of the contralateral ear in established unilateral Menière's disease. Laryngoscope 2004;114:1373–6.

[12] Cureoglu S, Schachern PA, Paul S, Paparella MM, Singh RK. Cellular changes of Reissner's membrane in Meniere's disease: human temporal bone study. Otolaryngol Head Neck Surg 2004;130:113–19.